

Article

Autonomous Modulation Categorization Algorithm for Amplify and Forward Relaying Diversity Systems

Mohamed Marey^{1,*}  and Hala Mostafa^{2,†} 

¹ Smart Systems Engineering Laboratory, College of Engineering, Prince Sultan University, Riyadh 11586, Saudi Arabia

² Department of Information Technology, College of Computer and Information Sciences, Princess Nourah bint Abdulrahman University, P.O. Box 84428, Riyadh 11671, Saudi Arabia; hmostafa@pnu.edu.sa

* Correspondence: mfmarey@psu.edu.sa

† These authors contributed equally to this work.

Abstract: Modulation categorization, which is a significant duty performed by smart receivers, is critical for applications in both the military and civilian sectors. This research topic has been intensively investigated for single-hop wireless communications. However, there are a few studies that concentrate on multiple hop communications systems. In this paper, we design a novel autonomous modulation categorization technique for amplify-and-forward relaying systems. Analytical formulations of correlation functions used as the foundation of the proposed method are developed. By exploiting the spatial redundancy, we theoretically demonstrate that a set of modulation forms produces peaks for particular correlation functions whereas the other set does not. We design a multiple-level hypothesis assessment for judgment based on this property. The suggested approach has the benefit of not requiring channel coefficients or noise power information. Computer simulations are conducted to test the proposed method's categorization performance. The findings demonstrate that the suggested method produces appropriate results under various operating situations. The suggested approach reaches an accuracy of about one hundred percent when the SNR is 10 dB or higher. On the other hand, the traditional algorithms fail to provide acceptable performance even at high SNR.

Keywords: modulation categorization; relaying diversity; adaptive transmissions



Citation: Marey, M.; Mostafa, H. Autonomous Modulation Categorization Algorithm for Amplify and Forward Relaying Diversity Systems. *Electronics* **2022**, *11*, 1899. <https://doi.org/10.3390/electronics11121899>

Academic Editor: Maysam Abbod

Received: 25 May 2022

Accepted: 11 June 2022

Published: 16 June 2022

Publisher's Note: MDPI stays neutral with regard to jurisdictional claims in published maps and institutional affiliations.



Copyright: © 2022 by the authors. Licensee MDPI, Basel, Switzerland. This article is an open access article distributed under the terms and conditions of the Creative Commons Attribution (CC BY) license (<https://creativecommons.org/licenses/by/4.0/>).

1. Introduction

Autonomous modulation categorization (AMC) is a signal processing tool that smart receivers employ to recognize the modulation forms of the signals they have received. This is necessary to guarantee that the received signals are demodulated correctly and that the broadcast data are accurately retrieved. This technology is deployed in a wide range of defense, government, and commercial applications [1–3].

The usage of AMC in military situations was the impetus for its creation where electronic warfare and threat analysis need the detection of the modulation form of a received signal to distinguish opponent transmitters, generate jamming signals, and recover the intercepted signal. In contemporary civilian applications, the transmitter may use a wide variety of modulation forms to regulate the data rate and the bandwidth utilization while maintaining a particular level of quality of service. The pool of modulation forms is known to both the sending and receiving nodes. However, the modulation form that is dynamically adjusted at the transmitter to accommodate channel circumstances may be unspecified to the receiver. As a result, there must be some kind of AMC mechanism at the receiving terminal in place to make sure that the received message is securely demodulated. This concept has recently been incorporated in several wireless commercial standards such as cellular devices, wireless local area networks, and microwave communication systems [4]. AMC is also adopted by government authorities for spectrum monitoring

in order to assure adherence to spectrum control standards. This guarantees that vital agencies such as security forces, fire departments, air navigation, and the military have access to reliable communications that are not hampered by outside influences.

Meanwhile, relaying diversity wireless communications have garnered considerable interest in academic and industrial sectors owing to their favorable performance features such as link reliability, system capacity, and transmission range, as well as the ease of implementation that they provide [5–7]. There are typically two rounds in a relaying transmission system. In the first round, the relay and destination receive data from the source. During the following round, the source is idle while the relay conveys the source's information to the destination. Simply, the relay link serves as a supplementary link to the main link that connects the source and destination. The processing of the message delivered from the originating node by the relay is a crucial component of the relaying diversity mechanism. Various processing strategies result in various relaying diversity protocols such as amplify-and-forward (AF), mixed-and-forward, compress-and-forward, and decode-and-forward [8,9]. AF is a straightforward technique, which utilizes a non-regenerative relay to transfer a scaled version of the incoming signal to the eventual destination.

This work addresses the AMC challenge in AF diversity systems. What follows is an outline of the remainder of the paper. Works that are relevant to this topic are explored in Section 2. The system model is discussed in Section 3. The correlation functions for various modulation types as well as the algorithm under consideration are covered in Sections 4 and 5. The simulation outcomes are presented in Section 6. The concluding findings are made in Section 7.

2. Related Works

One of the most widely used modulation categorization approaches is called likelihood-based, while the other is called feature-based [10–12]. The information necessary of the former approach is included in the probability density function of the sensed signal, conditioned on an embedded modulation scheme. Three likelihood technique variants are conceivable, depending on the model used for the unknown parameters such as synchronization and channel coefficients: average likelihood ratio test (ALRT), generalized likelihood ratio test (GLRT), and hybrid likelihood ratio test (HLRT) [13]. As a general rule, likelihood ratio tests fail to perform successfully when the received signal is influenced by transmission defects such as frequency and timing offsets [14]. To counteract this weakness, the latter class of feature-based techniques utilizes signal properties such as cyclostationary, signal statistics, wavelet transform, spectral features, and, zero-crossings to differentiate between the various modulation forms [15].

Substantial developments have been accomplished on AMC across a variety of single-hop transmissions, including single-input single-output, multiple antennas, single-carrier and multicarrier, as well as uncoded and coded wireless systems. The strengths and effectiveness of relaying diversity (multi-hop) transmissions, on the one side, and the relevance of AMC, on the other side, provide a very hot research topic. However, the problem of AMC for relaying systems remains comparatively unexplored. The reason is that the existence of two unknown wireless channels between the source and destination makes it difficult to execute AMC over relay transmissions. Recently, [16,17] have proposed two AMC algorithms over decode-and-forward two-path relaying systems. The primary distinction between our study and the methods described in [16,17] is illustrated Table 1.

Table 1. Comparative analysis of our study and existing works.

	Proposed Method	Method in [16]	Method in [17]
Number of relays	1	2	2
Relaying type	Amplify-and-forward	Decode-and-forward	Decode-and-forward
Cooperation type	Single path	Two paths	Two paths
Mode of operation	Blind	Blind	Data aided
Channel estimation	Not required	Required	Required
Packet size	Not required	Required	Required

A summary of the most important contributions of this research is provided in the following.

- This is the first research of its sort in the literature to provide an AMC method for amplify-and-forward (AF) relaying systems.
- The underlying structure of the received signals is utilized to mathematically create a family of correlation functions. Each one of these functions reveals spikes for a certain set of modulation schemes, but it shows nothing for other modulation schemes.
- In consideration of the aforementioned discovery attribute, a revolutionary judgment test that is predicated on the concept of a false alarm is designed.
- The proposed method has a variety of benefits, one of which is that it does not call for the channel state information or the noise power to be known.
- The proposed method can discriminate between any number of modulation schemes as long as there exist correlation functions that indicate spikes for some schemes and null for others.

3. System Model

Source S , relay R , and destination D are the three nodes of the two-hop relaying system shown in Figure 1. There is one antenna element on each node, and the relay functions in a half-duplex manner. The terminals R and D have the same additive white Gaussian noise (AWGN) variance of σ_n^2 . It is assumed that each connection has a flat-frequency response, and the channel coefficient between nodes α and β is represented by the symbol $h_{\alpha\beta}$ where $\alpha \in \{S, R\}$ and $\beta \in \{R, D\}$. The signal that comes via the $S - D$ link is not minor at all; nonetheless, it is used as an additional channel in order to improve the system performance. There are a number of B bits included in each frame of transmission. The transmission is broken up into two time slots.

First time slot

The modulator of the source converts each successive m bits into a specific symbol $d(n)$ belonging to the $|\Omega|$ -point constellation Ω , where n is the symbol index. The modulator's output is expressed by a frame of N data symbols, $\mathbf{d} = [d(0), \dots, d(N-1)]$, where $N = B/m$. The assigned modulation form Ω is carefully picked from a list of established options to ensure compatibility with the link's specifications. The relay and the destination nodes receive the source's frame through $S - R$ and $S - D$ links, respectively. Mathematically, we formulate the n th received signals at the relay, $y_R(n)$, and the destination, $y_D^{(1)}(n)$, respectively, as

$$y_R(n) = h_{SR}d(n) + w_R(n), \quad (1)$$

and

$$y_D^{(1)}(n) = h_{SD}d(n) + w_D^{(1)}(n), \quad (2)$$

where $w_R(n)$ and $w_D^{(1)}(n)$ represent AWGN components at the relay and the destination, respectively, and $n = 0, 1, \dots, N$.

Second time slot

The relay magnifies the incoming signal and sends it on to the destination node. The received signal at the destination node is expressed as

$$y_D^{(2)}(n) = Ah_{RD}y_R(n) + w_D^{(2)}(n), \tag{3}$$

where A is the amplification factor, and it is given as [9]

$$A = \frac{1}{\sqrt{|h_{SR}|^2 + \sigma_n^2}}.$$

As a result, the relay’s output power remains the same as the source’s output power. Using (1) into (3), we re-write $y_D^{(2)}(n)$ as

$$y_D^{(2)}(n) = Ah_{RD}h_{SR}d(n) + Ah_{RD}w_R(n) + w_D^{(2)}(n). \tag{4}$$

The purpose of this study is to create a strategy for identifying the assigned modulation form Ω by making use of characteristics retrieved from the signals $y_D^{(1)}(n)$ and $y_D^{(2)}(n)$, $n = 0, \dots, N - 1$, that were received in two time slots.

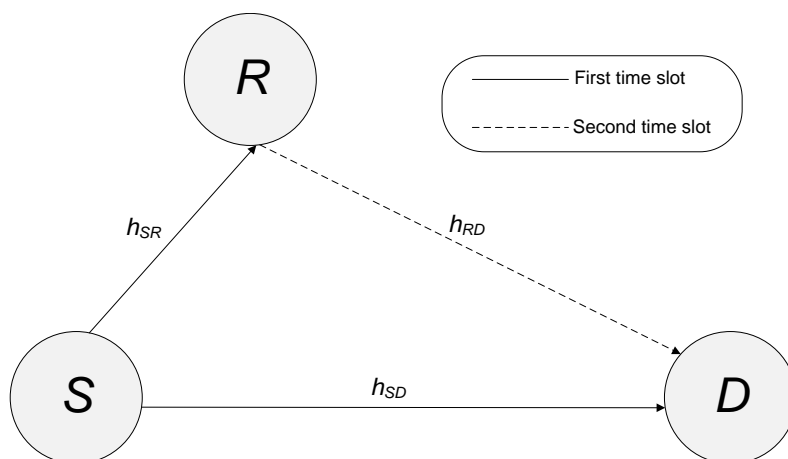


Figure 1. Relaying system including source S , relay R , and destination D nodes.

4. Statistical Properties of the Received Signal

The statistical aspects of received signals are examined in this section with the goal of discovering features that may be leveraged to categorize the modulation form used in the transmission. Throughout the exploration, we are going to assume the following.

- There is no correlation between $d(n_1)$ and $d(n_2)$:

$$E[d(n_1)d(n_2)] = \begin{cases} \delta(n_1 - n_2) & \text{for } \Omega = \text{BPSK} \\ 0 & \text{Otherwise,} \end{cases} \tag{5}$$

where $E[\cdot]$ is the statistical expectation of a random variable, $\delta(\cdot)$ is the Kronecker delta function, and BPSK denotes to a binary phase shift keying constellation. Furthermore,

$$E[d(n_1)d(n_2)] = \delta(n_1 - n_2), \tag{6}$$

for all possible values of Ω belong to the constellation options of M -PSK and M -QAM. Here $*$ indicates the complex conjugate operator and M is the modulation order. Here, without loss of generality, we assume that the signal power is one.

- The data symbols are uncorrelated with the noise samples:

$$\begin{aligned} E[d(n_1)w_R(n_2)] &= E[d(n_1)w_R^*(n_2)] = 0, \\ E[d(n_1)w_D(n_2)] &= E[d(n_1)w_D^*(n_2)] = 0. \end{aligned} \tag{7}$$

- The noise samples are uncorrelated with each other:

$$\begin{aligned} E[w_R(n_1)w_D^{(1)}(n_2)] &= E[w_R(n_1)w_D^{(2)}(n_2)] = 0, \\ E[w_R(n_1)w_D^{(1)*}(n_2)] &= E[w_R(n_1)w_D^{(2)*}(n_2)] = 0, \\ E[w_D^{(1)}(n_1)w_D^{(2)}(n_2)] &= 0, \\ E[w_D^{(1)}(n_1)w_D^{(2)*}(n_2)] &= E[w_D^{(1)}(n_1)w_D^{(2)*}(n_2)] = 0. \end{aligned} \tag{8}$$

- The channel coefficients are unknown random variables.

We describe the following correlation functions:

$$U_1(n_1, n_2) = E[y_D^{(1)}(n_1)y_D^{(2)}(n_2)], \tag{9a}$$

$$U_2(n_1, n_2) = E[y_D^{(1)}(n_1)(y_D^{(2)}(n_2))^3], \tag{9b}$$

$$U_3(n_1, n_2) = E[y_D^{(1)}(n_1)(y_D^{(2)}(n_2))^7], \tag{9c}$$

and

$$U_4(n_1, n_2) = E[(y_D^{(1)}(n_1))^4(y_D^{(2)*}(n_2))^2]. \tag{9d}$$

After a straightforward computations based on the aforementioned assumptions and prior correlation functions, we write

$$U_1(n_1, n_2) = \begin{cases} Ah_{SR}h_{RD}h_{SD}\delta(n_1 - n_2) & \text{for } \Omega = \text{BPSK} \\ 0 & \text{otherwise,} \end{cases} \tag{10a}$$

$$U_2(n_1, n_2) = \begin{cases} A^3h_{SR}^3h_{RD}^3h_{SD}\delta(n_1 - n_2) & \text{for } \Omega = \text{BPSK, QPSK,} \\ -0.68A^3h_{SR}^3h_{RD}^3h_{SD}\delta(n_1 - n_2) & \text{for } \Omega = \text{16-QAM,} \\ -0.619A^3h_{SR}^3h_{RD}^3h_{SD}\delta(n_1 - n_2) & \text{for } \Omega = \text{64-QAM,} \\ 0 & \text{for } \Omega = \text{8-PSK, 16-PSK,} \end{cases} \tag{10b}$$

$$U_3(n_1, n_2) = \begin{cases} A^7h_{SR}^7h_{RD}^7h_{SD}\delta(n_1 - n_2) & \text{for } \Omega = \text{BPSK, QPSK, 8-PSK} \\ 2.2A^7h_{SR}^7h_{RD}^7h_{SD}\delta(n_1 - n_2) & \text{for } \Omega = \text{16-QAM,} \\ 1.91A^7h_{SR}^7h_{RD}^7h_{SD}\delta(n_1 - n_2) & \text{for } \Omega = \text{64-QAM,} \\ 0 & \text{for } \Omega = \text{16-PSK,} \end{cases} \tag{10c}$$

and

$$U_4(n_1, n_2) = \begin{cases} A^2(h_{SR}^*h_{RD}^*)^2h_{SD}^4\delta(n_1 - n_2) & \text{for } \Omega = \text{BPSK, QPSK,} \\ 0 & \text{for } \Omega = \text{8-PSK, 16-PSK, 16-QAM, 64-QAM.} \end{cases} \tag{10d}$$

Snapshots of correlation functions magnitudes for various modulation forms are shown in Figures 2–5 at a signal-to-noise (SNR) ratio of 20 dB and a number of symbol per frame of 5000. The channel parameters are specified as provided in Section 6. These findings are in agreement with the theoretical conclusions drawn earlier. In practice, the limited observation window causes nonzero peaks to occur at places where zeros should exist. However, these are statistically negligible over a long observation period.

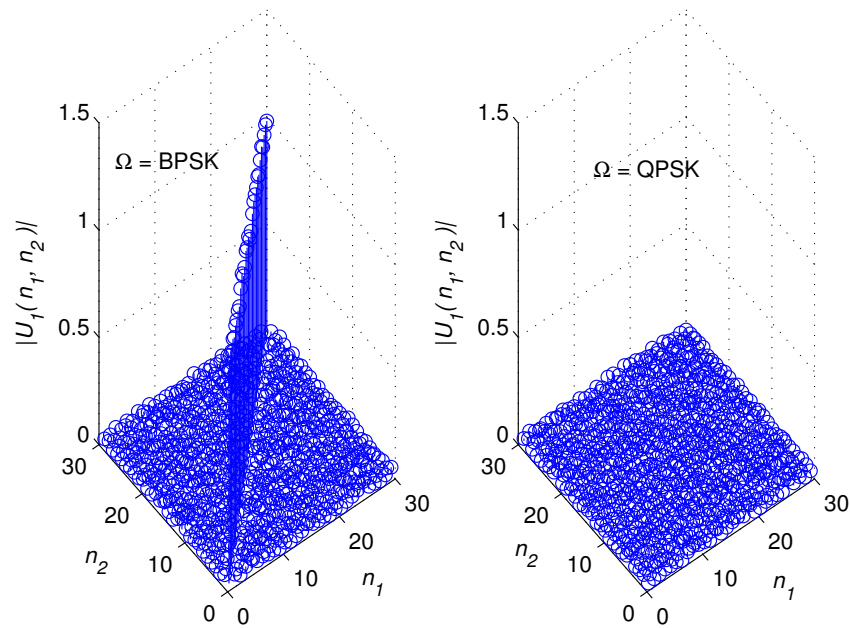


Figure 2. The magnitude of the first correlation function at the modulation forms of BPSK and QPSK.

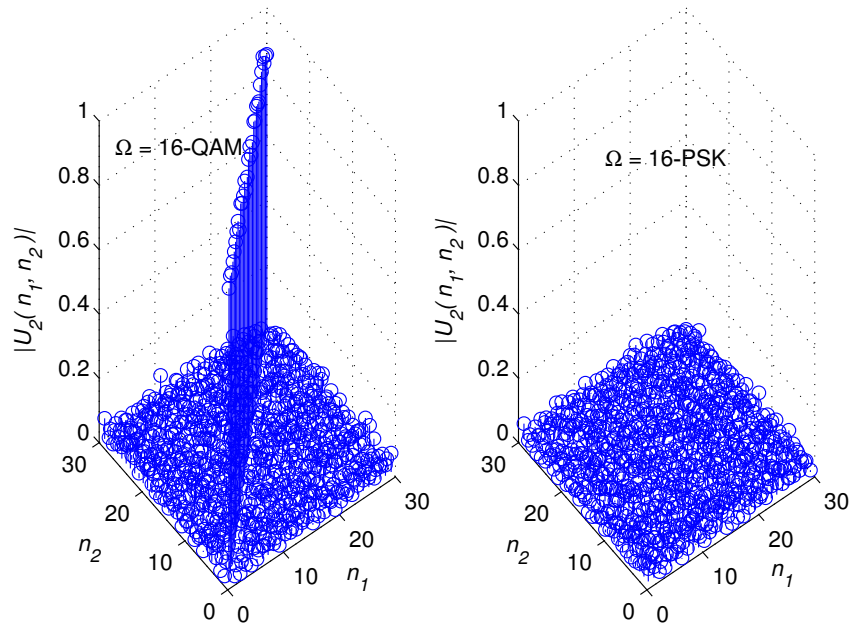


Figure 3. The magnitude of the second correlation function at the modulation forms of 16-QAM and 16-PSK.

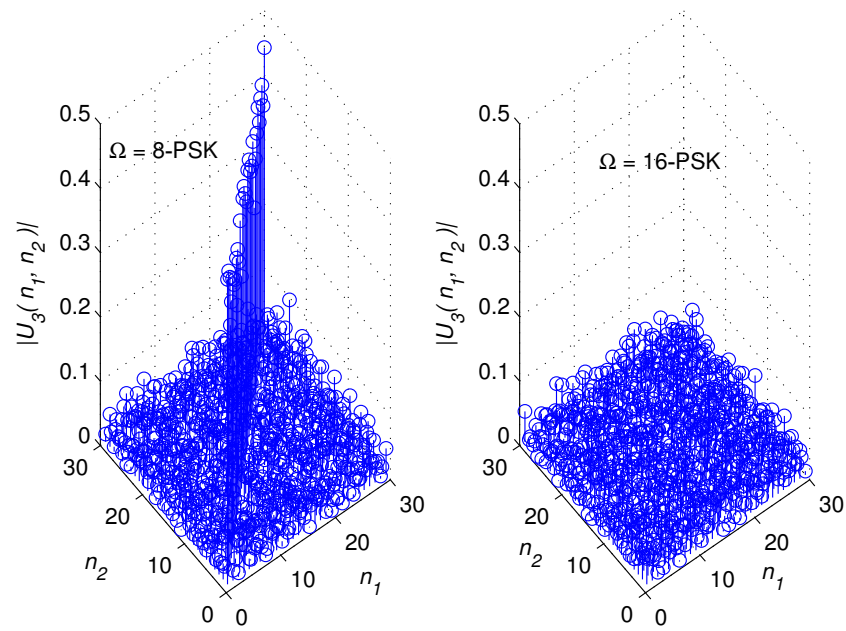


Figure 4. The magnitude of the third correlation function at the modulation forms of 8-PSK and 16-PSK.

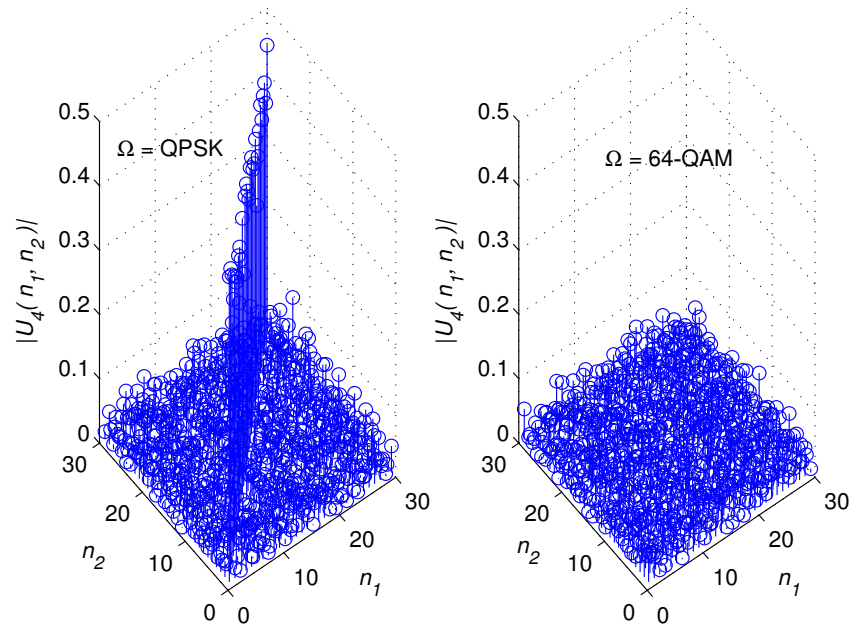


Figure 5. The magnitude of the fourth correlation function at the modulation forms of QPSK and 64-QAM.

5. Proposed Algorithm

As previously stated, the peaks of the specified correlation functions vary depending on the used modulation forms. We use this property in a binary decision tree approach to perform modulation categorization. Here, we propose a new peak identification technique that may be employed at each branch node in the graph. We define the method in a generic form in order to be consistent with any correlation function. The estimated value of a correlation function, denoted by the symbol G , is equal to

$$\hat{G} = \frac{1}{N} \sum_{n=0}^{N-1} f(y_D^{(1)}(n), y_D^{(2)}(n)), \tag{11}$$

where

$$f(y_D^{(1)}(n), y_D^{(2)}(n)) = \begin{cases} y_D^{(1)}(n)y_D^{(2)}(n) & \text{if } G = U_1(n, n) \\ y_D^{(1)}(n)(y_D^{(2)}(n))^3 & \text{if } G = U_2(n, n) \\ y_D^{(1)}(n)(y_D^{(2)}(n))^7 & \text{if } G = U_3(n, n) \\ (y_D^{(1)}(n))^4(y_D^{(2)*}(n))^2 & \text{if } G = U_4(n, n). \end{cases} \quad (12)$$

Note that in (11) and (12), we estimate the average value of the correlation function under consideration at $n_1 = n_2 = n$. This value reflects $P + \epsilon$ for certain modulation types and ϵ for others with P representing the corresponding peak value and ϵ being the estimation error, which includes the contribution of channel noise as well as estimation imperfection due to using a limited number of samples. There are two possible hypotheses to be examined:

$$\begin{aligned} \mathcal{H}_0 : \hat{G} &= \epsilon, \\ \mathcal{H}_1 : \hat{G} &= P + \epsilon, \end{aligned} \quad (13)$$

where hypotheses \mathcal{H}_1 and \mathcal{H}_0 refer to whether or not there was a peak. An optimum peak detector must have access to information about the channels that are not known. A method built on the false alarm rate notion is proposed to compensate for this information gap. Given hypothesis \mathcal{H}_0 and supposing that ϵ is a Gaussian random variable with zero-mean and variance $2\sigma^2$, it implies that $|\hat{G}| = |\epsilon|$ is a Rayleigh random variable, with mean $(\pi\sigma^2)/2$ and cumulative distribution function (CDF) provided by

$$C(z) = 1 - \exp(-z^2/2\sigma^2), \quad z \geq 0. \quad (14)$$

The core notion of the algorithm is to define a threshold ϕ , and the peak is reported existent if $|\hat{G}| \geq \phi$; otherwise, there is not a peak. Our goal is to attain a certain degree of false alarm probability (P_f), which is defined as the chance of falsely reporting the existence of peak. As a result, one may compose

$$P_f = \Pr(\hat{G} \geq \phi | \mathcal{H}_0) = 1 - C(\phi). \quad (15)$$

By inserting (14) into (15), we can get

$$\phi = \sqrt{2\sigma^2 \ln \frac{1}{P_f}}. \quad (16)$$

It is evident from (16) that in order to compute ϕ , one has to know the value of σ^2 . We predict σ^2 by processing the samples of $y_D^{(1)}(n)$ and $y_D^{(2)}(n)$ as

$$L = \left| \frac{1}{N(N-1)} \sum_{\substack{n_1, n_2 = 0, \\ n_1 \neq n_2}}^{N-1} f(y_D^{(1)}(n_1), y_D^{(2)}(n_2)) \right|, \quad (17)$$

where $f(y_D^{(1)}(n), y_D^{(2)}(n))$ is described in (12). Given that L is a Rayleigh random variable with a mean of $\sigma\sqrt{\pi}/2$, the predicted value σ^2 can be estimated as

$$\hat{\sigma}^2 = \frac{2L^2}{\pi}. \quad (18)$$

The flowchart in Figure 6 summarizes the proposed peak detection method.

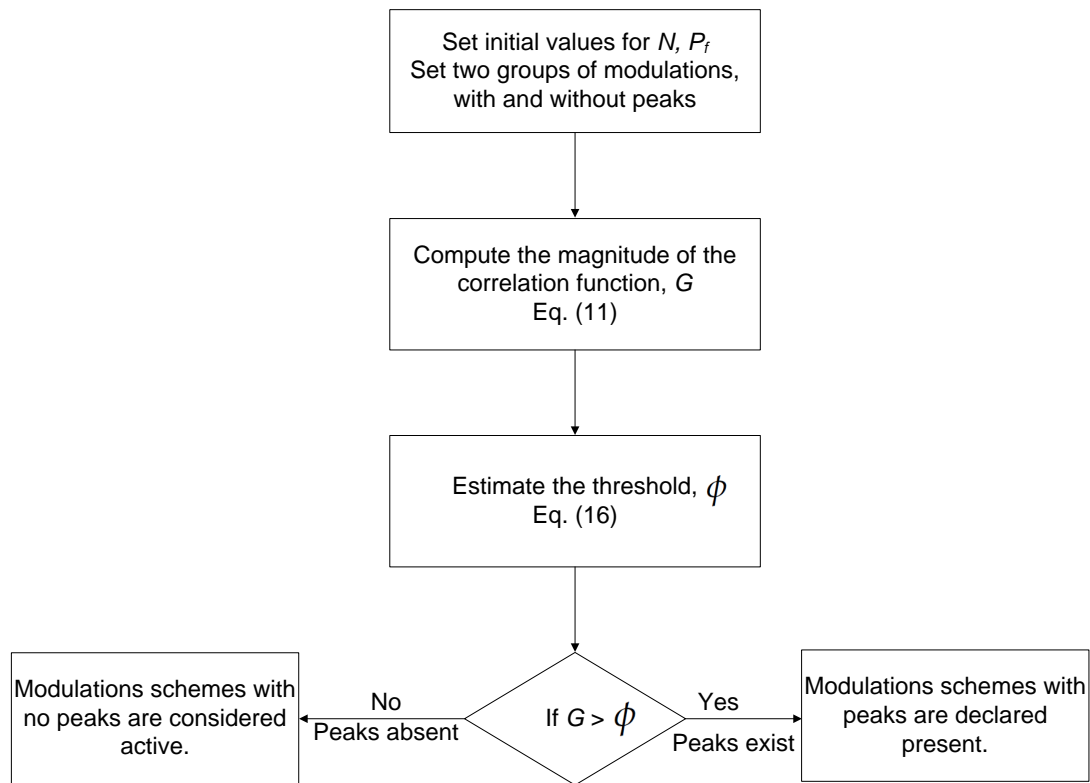


Figure 6. A summary of the proposed peak detection-method.

6. Simulation Results

Computer simulations have been used to examine the suggested algorithm's performance. We have used the sequential Monte Carlo simulation approach. Except when otherwise specified, the parameters of the system are: the number of symbol per frame $N = 5000$ and the probability of false alarm $P_f = 0.01$. The channel tap is described for each transmission link as a zero-mean complex-valued Gaussian random variable. The variance of each link is provided by

$$E \left[|h_{\alpha\beta}|^2 \right] = \left(\frac{v_{SD}}{v_{\alpha\beta}} \right)^\lambda, \quad (19)$$

where $\alpha \in \{S, R\}$ and β, λ is the path-loss exponent, $v_{\alpha\beta}$ is the distance between terminals α and β , and v_{SD} is the distance between terminals S and D . For the sake of the simulation, we assign $\lambda = 3.6$, $v_{SD} = 1$, $v_{SR} = 0.54$, and $v_{RD} = 0.55$. It is important to keep in mind that all distances have been normalized to v_{SD} . The probability of correct categorization, $P_c(\Omega = \rho|\rho)$, is utilized as a quality factor for the proposed algorithm, where ρ is one of the modulation kinds. Four distinct sets of modulation forms are investigated: $\Omega_1 = \{\text{BPSK, QPSK}\}$, $\Omega_2 = \{\text{BPSK, QPSK, 8-PSK}\}$, $\Omega_3 = \{\text{QPSK, 16-PSK, 16-QAM}\}$, and $\Omega_4 = \{\text{BPSK, QAM, 8-PSK, 64-QAM}\}$. The corresponding flowcharts for those sets are shown in Figure 7. The number of simulation trials was 1000.

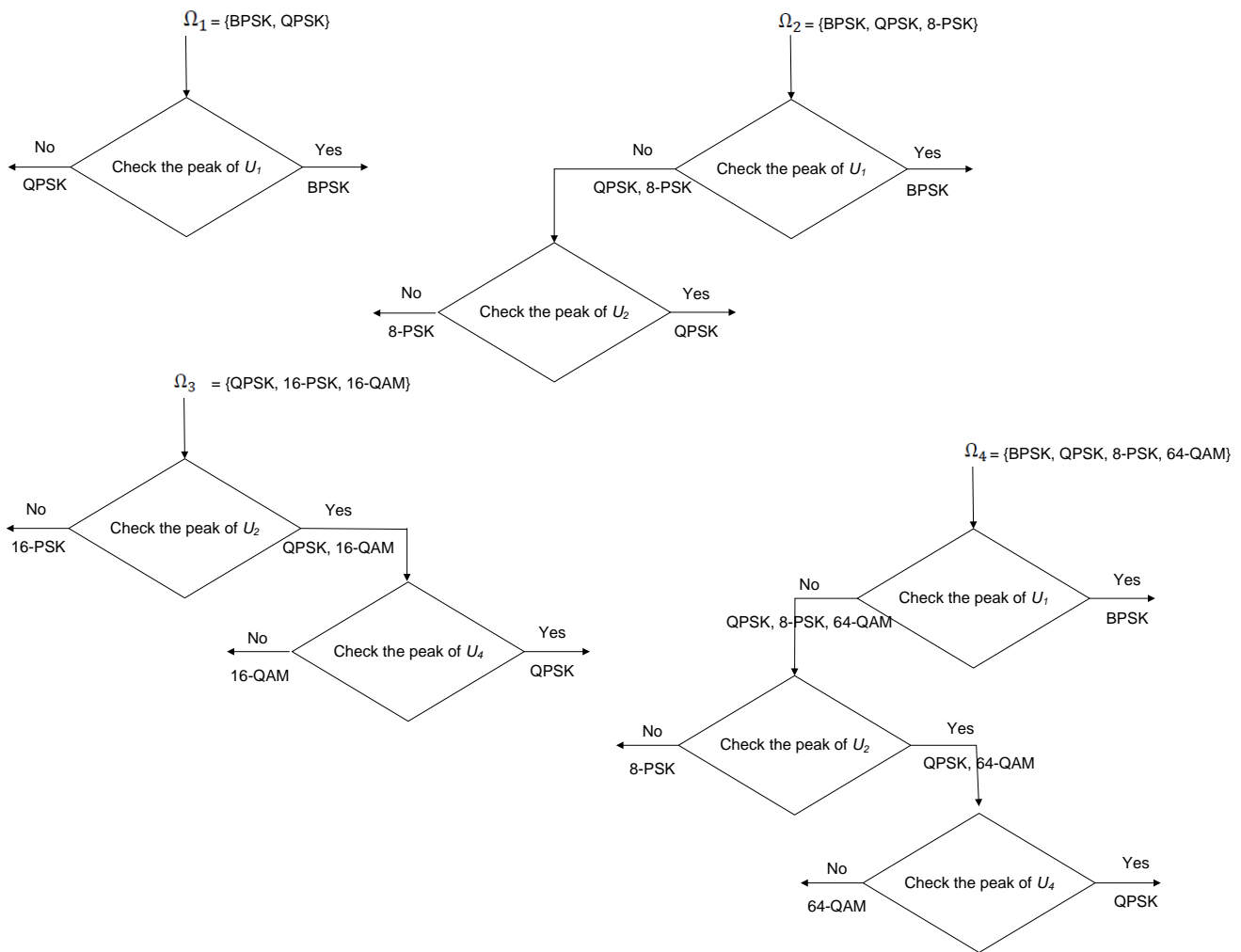


Figure 7. The flowcharts of four modulation sets.

Figures 8–11 illustrate the categorization performance for the modulation sets of Ω_1 , Ω_2 , Ω_3 , and Ω_4 , respectively, at different values of SNR. The findings indicate that the categorization performance of QPSK, 8-PSK, 16-PSK, 8-PSK of Figures 8–11, respectively, are not affected by SNR levels. This is due to the fact that their performance is governed by the likelihood of false alert, which was set at 0.01. However, the other modulation options show substantial improvements as SNR increases. This is because, when SNR levels increase, the peak detection performance improves.

Figures 12–15 examine the implication of the probability of false alarm on the categorization performance for Ω_1 , Ω_2 , Ω_3 , and Ω_4 , respectively. The findings reveal that when SNR increases, the performance reliance of modulations that display peaks on P_f reduces. The rationale is that with greater SNR, the influence of noise contribution declines and performance is mostly determined by the estimate error caused by employing a limited observation interval. This error disappears as the observation time approaches infinity. In principle, reducing P_f leads to a decrease in the threshold level, which increases the peak detection efficiency. On the other hand, the opposite is true for none peak detection. As a result, P_f is set to accomplish a performance balance for peak and none-peak categorization.

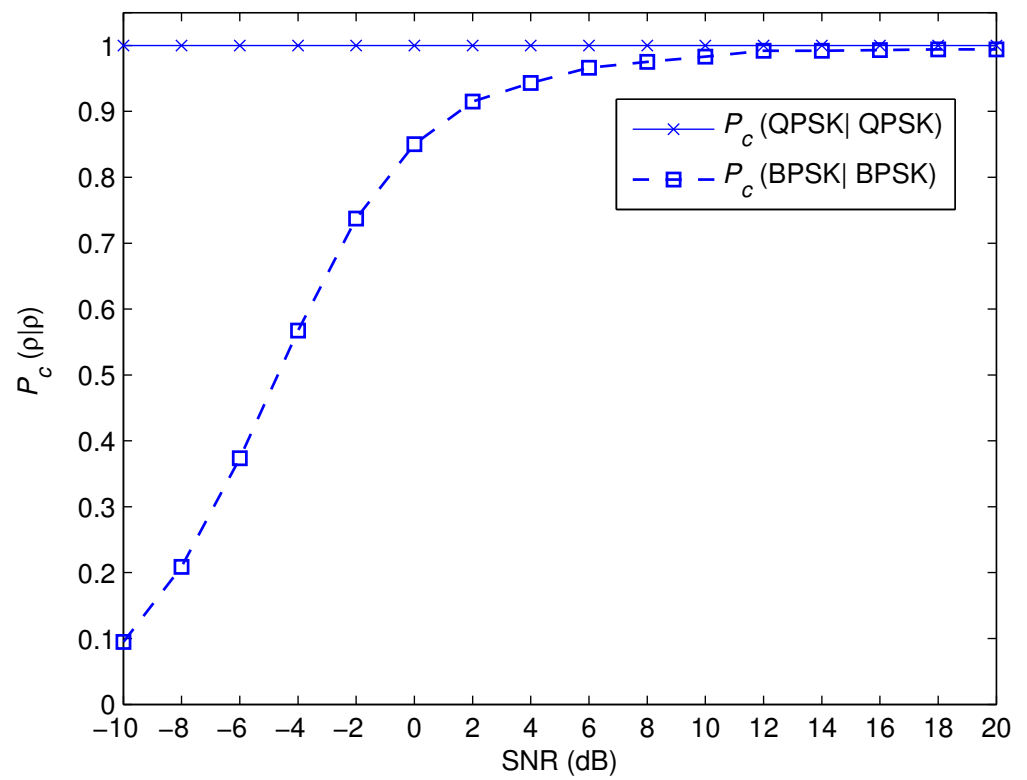


Figure 8. The categorization performance for the modulation set of Ω_1 .

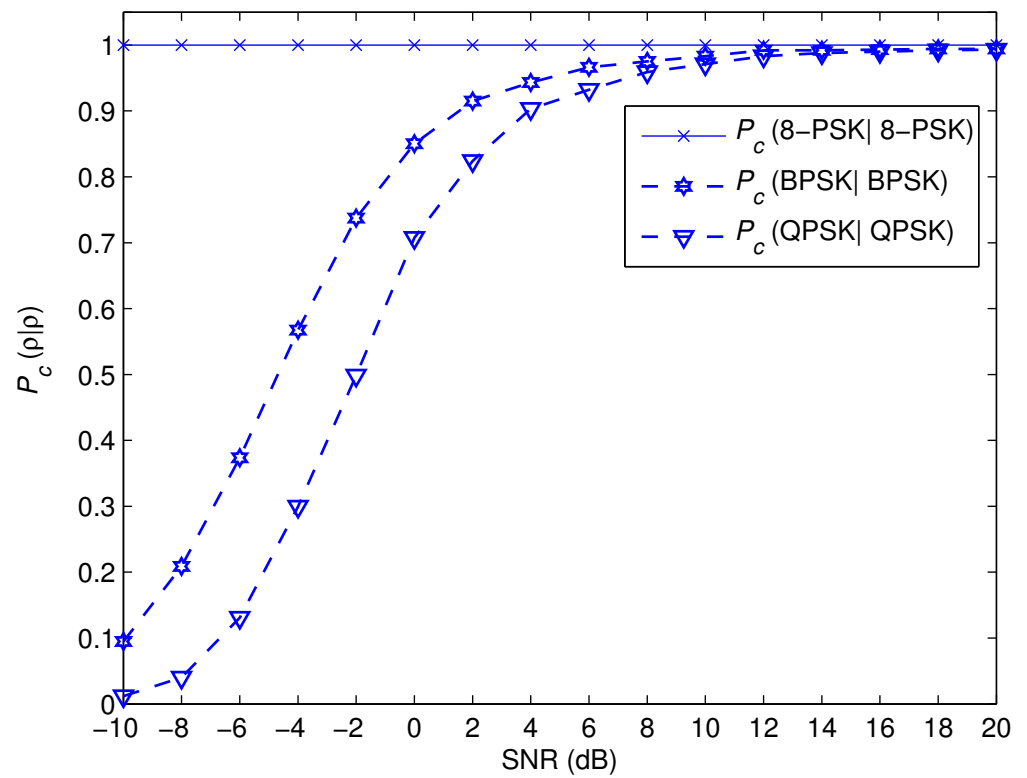


Figure 9. The categorization performance for the modulation set of Ω_2 .

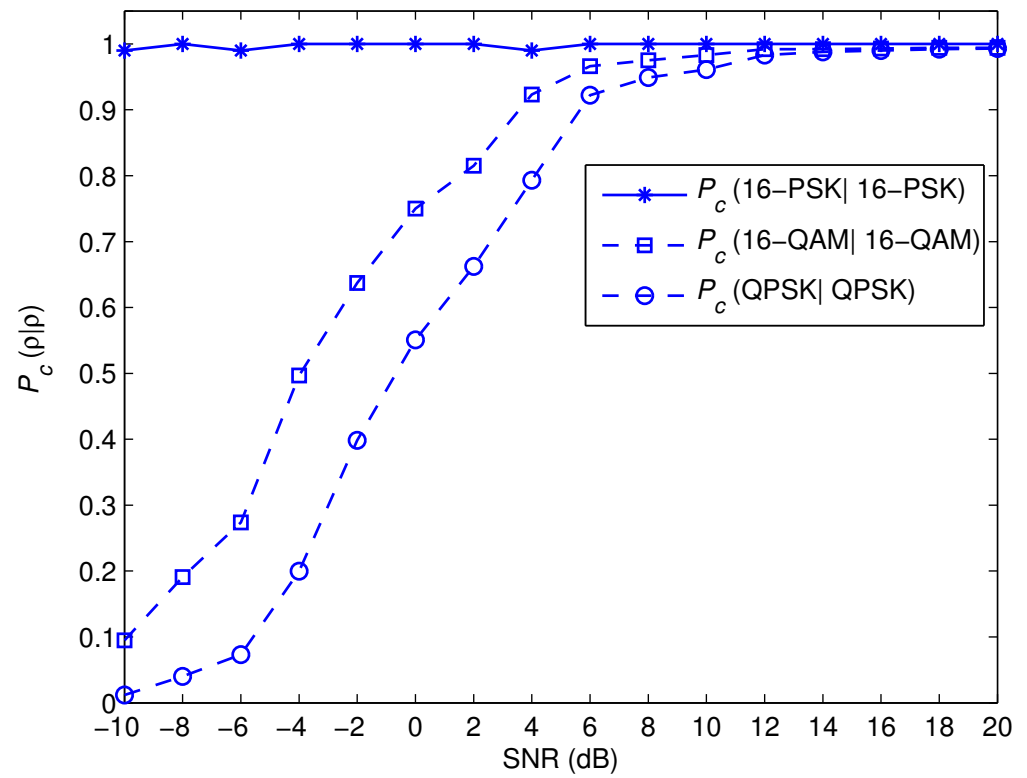


Figure 10. The categorization performance for the modulation set of Ω_3 .

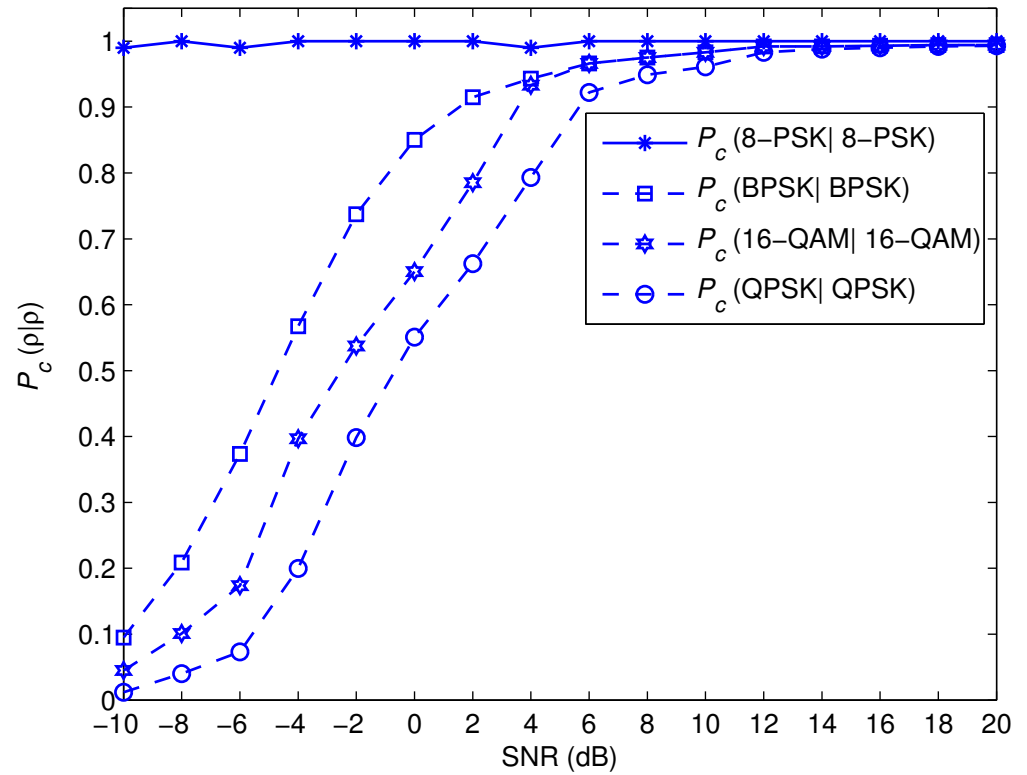


Figure 11. The categorization performance for the modulation set of Ω_4 .

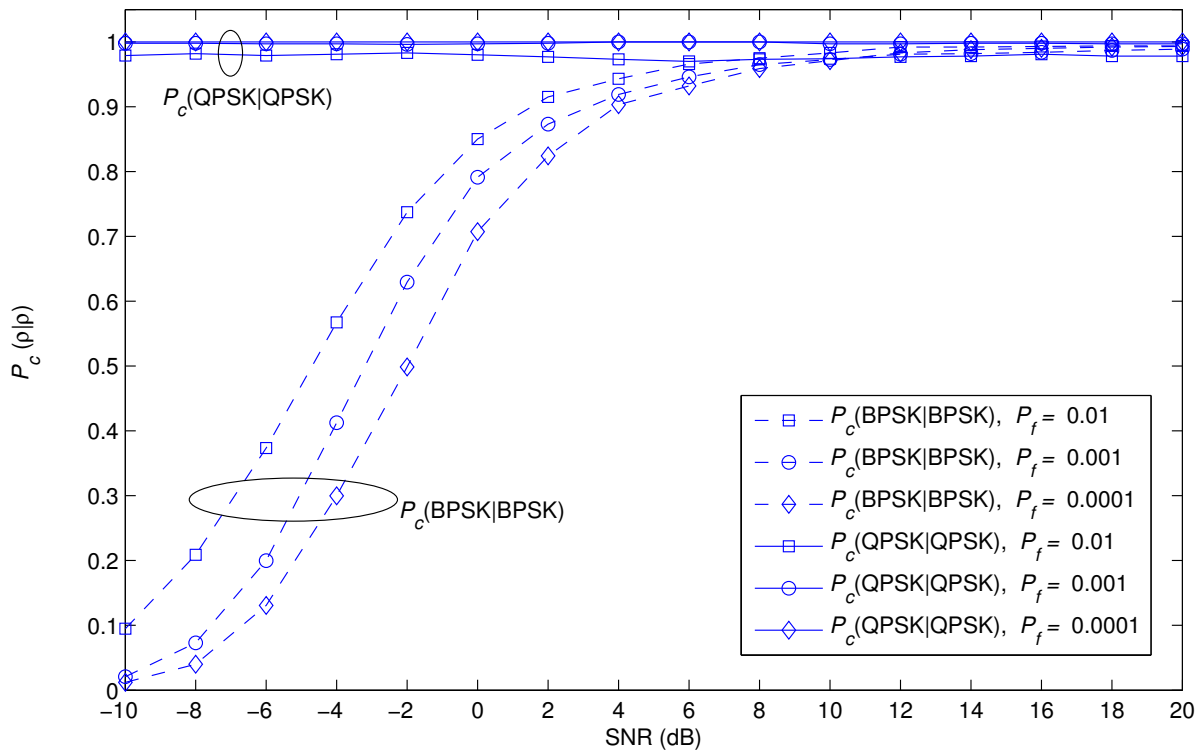


Figure 12. The effect of P_f on the categorization performance for the modulation set of Ω_1 .

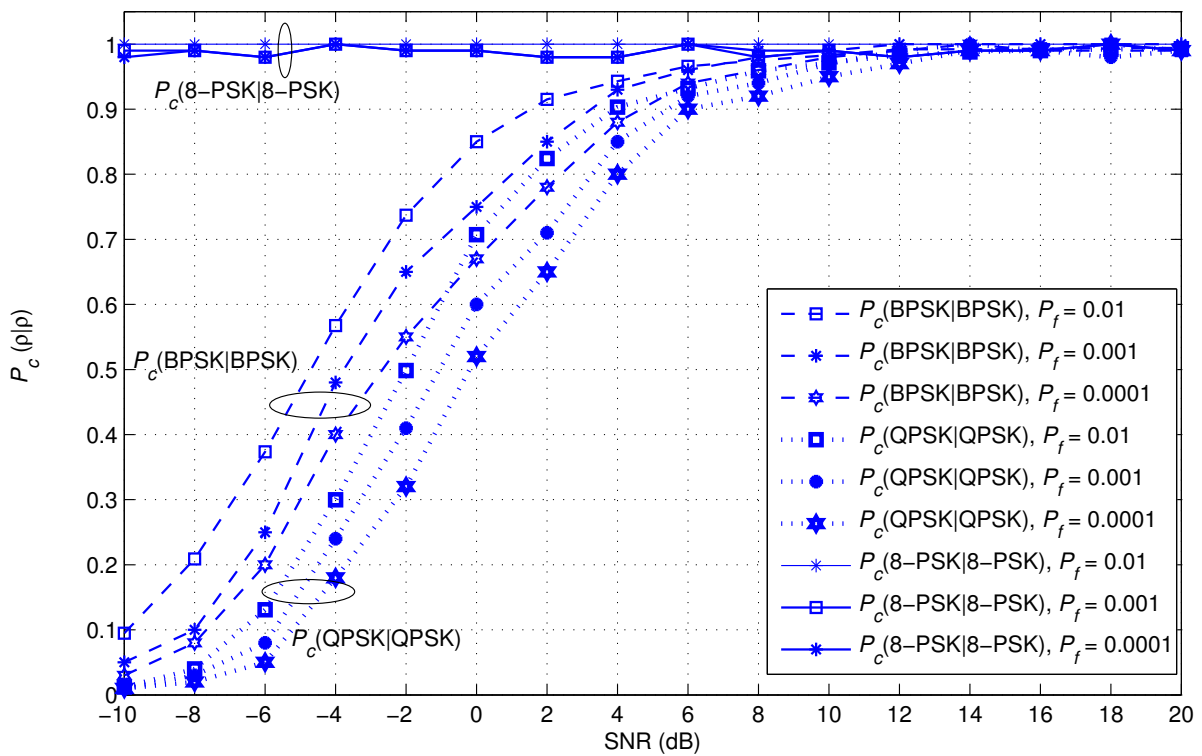


Figure 13. The effect of P_f on the categorization performance for the modulation set of Ω_2 .

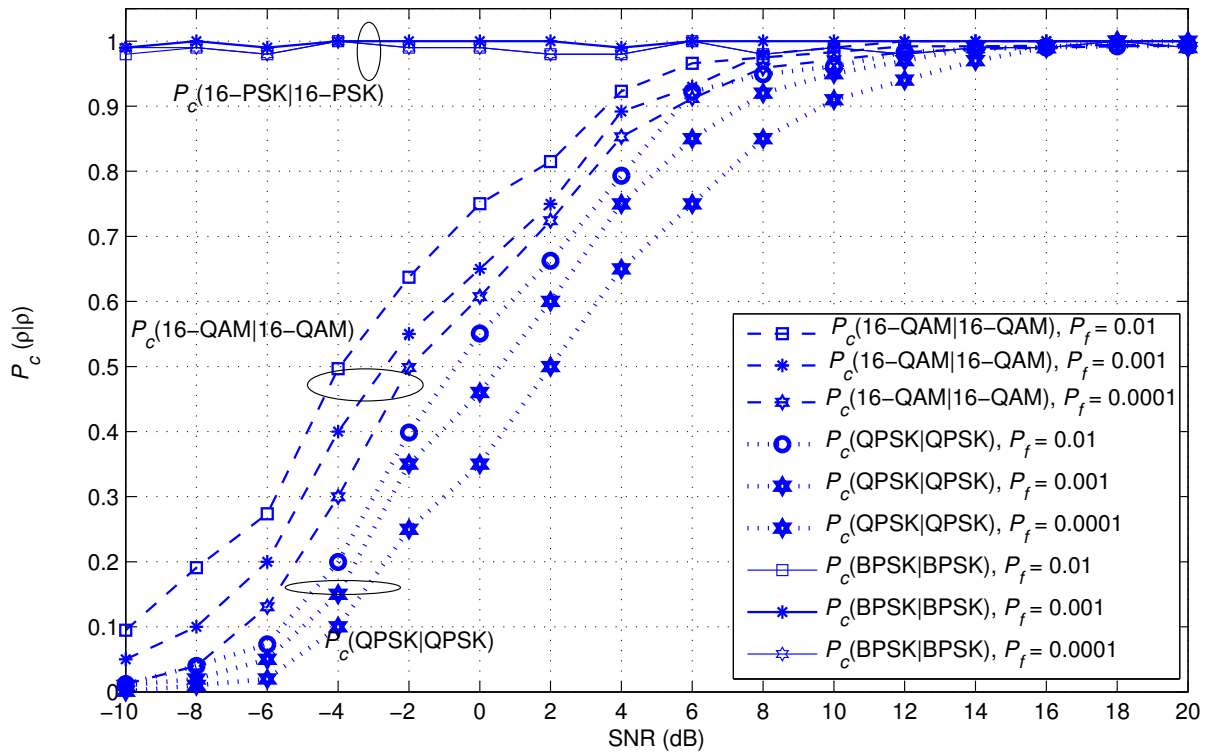


Figure 14. The effect of P_f on the categorization performance for the modulation set of Ω_3 .

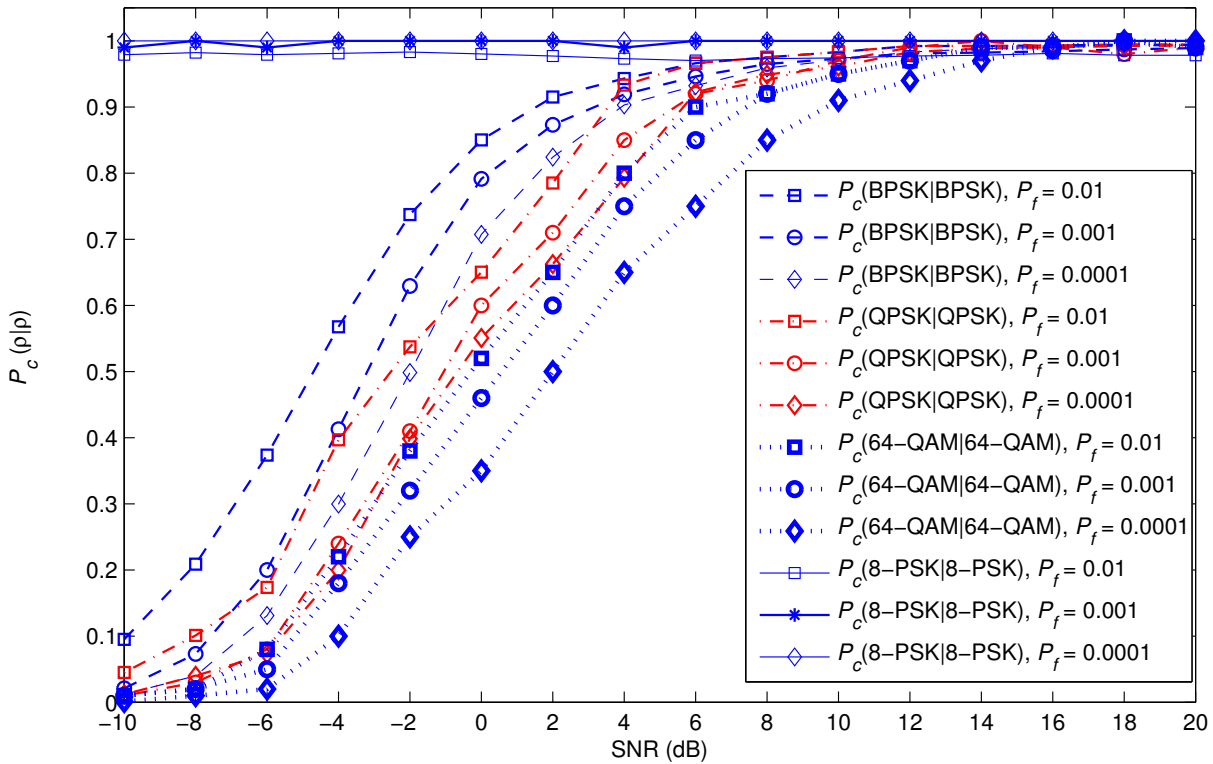


Figure 15. The effect of P_f on the categorization performance for the modulation set of Ω_4 .

Figures 16–19 display the impact of the number of symbols per frame, N , on the average likelihood of categorization, $P_A = \sum_{\rho} P_c(\Omega = \rho|\rho)$, for $\Omega = \Omega_1, \Omega_2, \Omega_3$, and Ω_4 , respectively. Increasing N even at moderate or low SNR levels leads to a considerable

enhancement. This demonstrates how the impact of the estimating inaccuracy lessens as the number of observations increases. Even with a high signal-to-noise ratio, an unsatisfactory level of categorization performance is reached when N is sufficiently low to allow the influence of estimate error to predominate.

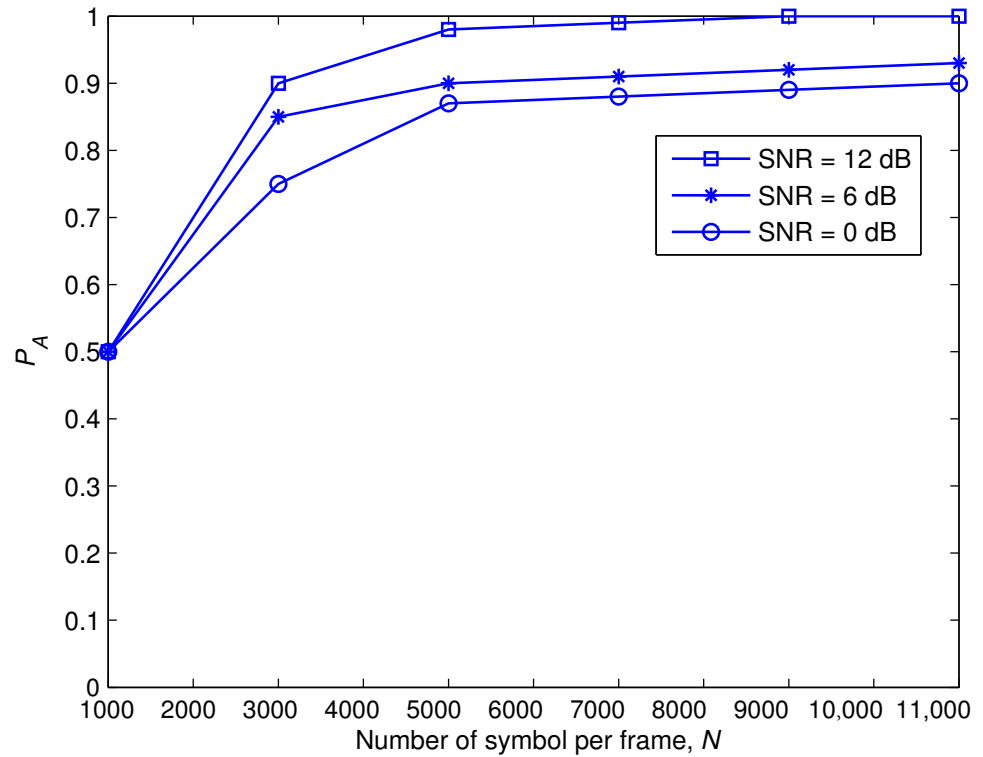


Figure 16. The effect of N on the categorization performance for the modulation set of Ω_1 .

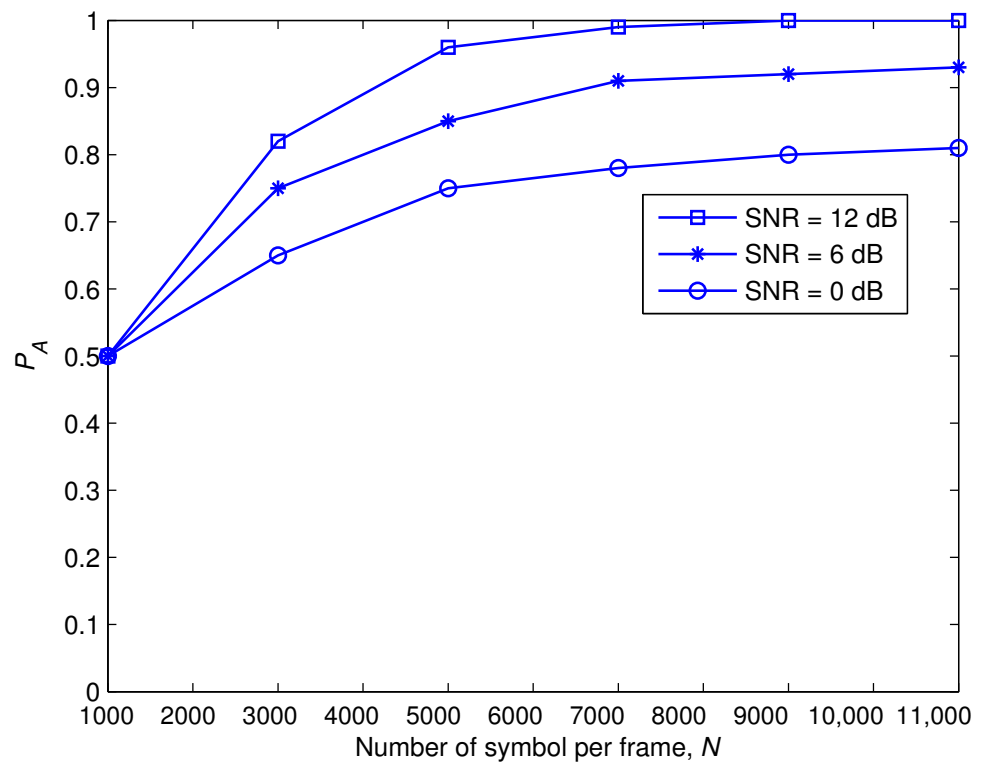


Figure 17. The effect of N on the categorization performance for the modulation set of Ω_2 .

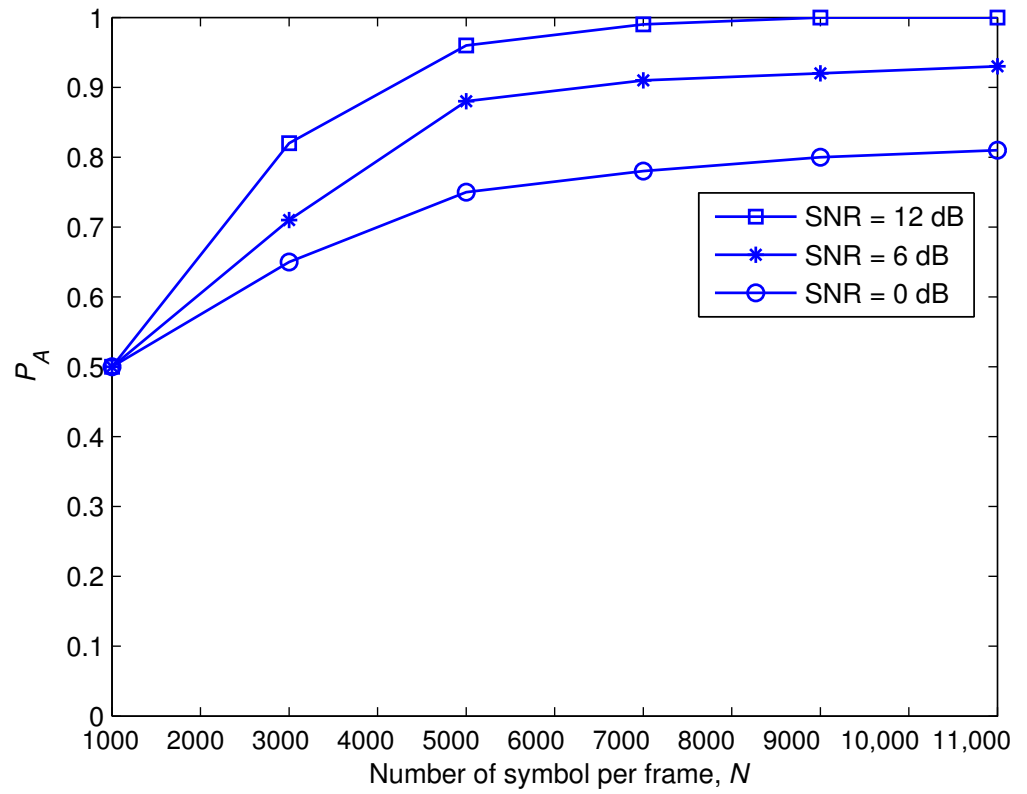


Figure 18. The effect of N on the categorization performance for the modulation set of Ω_3 .

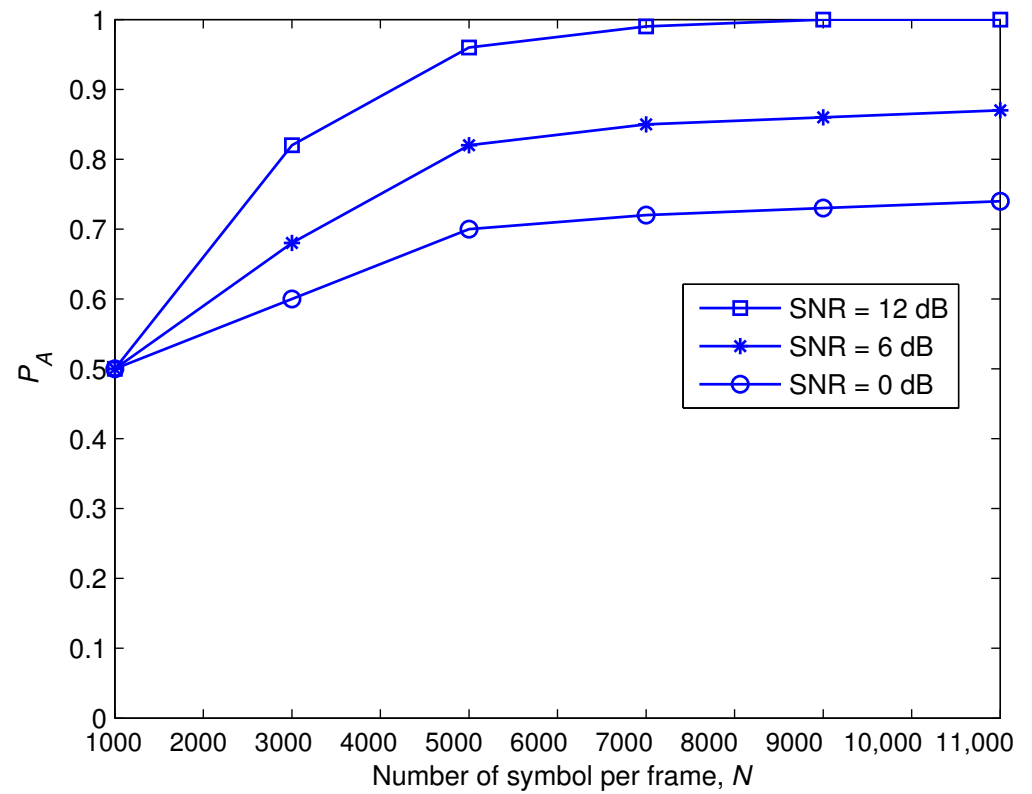


Figure 19. The effect of N on the categorization performance, for the modulation set of Ω_4 .

Figure 20 illustrates a comparison between the performance of the algorithm that is suggested and the performance of two other algorithms that were recently presented in [16,17]. The results show that the suggested method is superior to other algorithms. Even at high SNR levels, the other methods fail to provide good results. However, the suggested method provides almost perfect categorization performance. Recall that such methods are intended to function under the premise of channel coefficients and packet length knowledge; however, the suggested method does not.

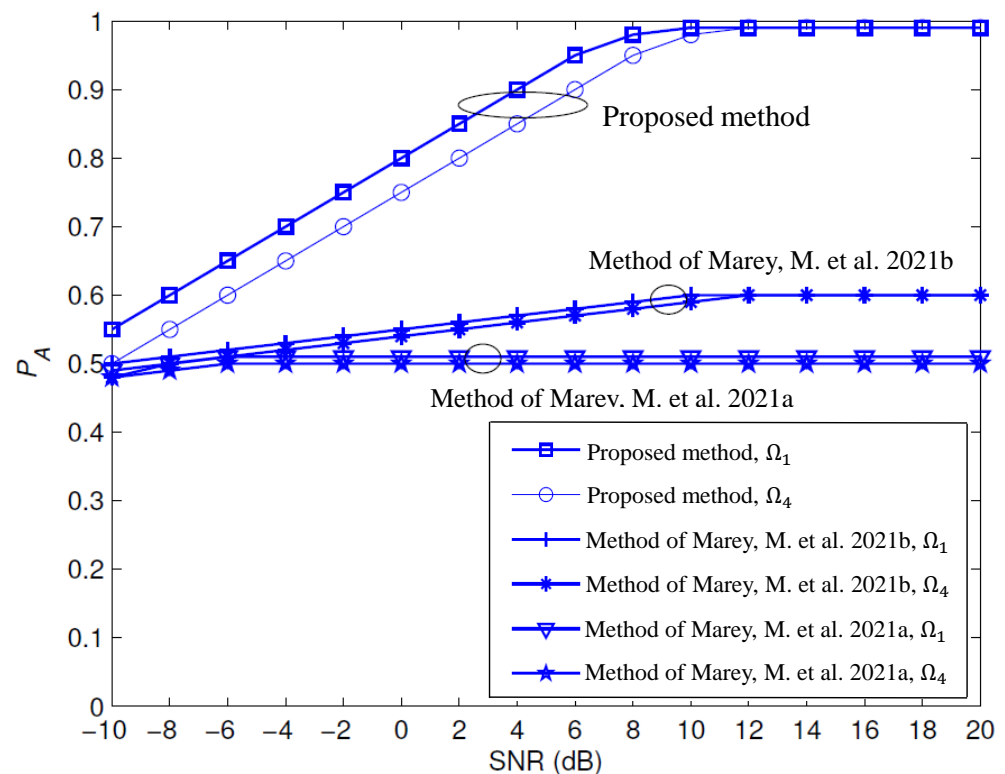


Figure 20. The performance of the proposed method in comparison to previous works for the modulation sets of Ω_1 and Ω_4 [16,17].

7. Conclusions

During this investigation, the problem of modulation categorization for amplify-and-forward relaying systems was examined. A number of correlation functions were presented to lay the foundations for the proposed technique. For certain modulation types, analytical derivations and simulation findings illustrated fixed position peaks in the correlation functions, whereas no such peaks could be found for the other forms of modulation. This finding was adopted as a feature selection. Based on the false-alarm criteria, we developed a binary tree method for peak recognition. The simulation results demonstrated outstanding categorization performance under a variety of operational situations. The proposed method achieved a precision of around one hundred percent when the SNR was at least 10 dB. Furthermore, increasing the number of samples processed beyond 5000 did not improve the performance of the proposed method noticeably. When the SNR was less than 6 dB, boosting the false alarm rate greatly increased the overall performance, but it did not make much of a difference when the SNR was greater. On the other hand, the previously reported algorithms were below 60 percent accurate at high SNR levels, which is not good enough for real-world use. These wonderful outcomes were obtained without previous awareness of channel status information or noise power.

Author Contributions: Conceptualization, M.M. and H.M.; methodology, M.M. and H.M.; software, M.M. and H.M.; validation, M.M. and H.M.; formal analysis, M.M. and H.M.; investigation, M.M. and

H.M.; resources, M.M. and H.M.; data creation, M.M. and H.M.; writing—original draft preparation, M.M. and H.M.; writing—review and editing, M.M. and H.M.; visualization, M.M. and H.M.; supervision, M.M. and H.M.; project administration, M.M. and H.M.; funding acquisition, M.M. and H.M. All authors have read and agreed to the published version of the manuscript.

Funding: Princess Nourah bint Abdulrahman University Researchers Supporting Project number (PNURSP2022R137), Princess Nourah bint Abdulrahman University, Riyadh, Saudi Arabia. The authors would like to acknowledge the support of Prince Sultan University for paying the Article Processing Charges (APC) of this publication.

Conflicts of Interest: The authors declare no conflict of interest.

References

1. Dobre, O.A. Signal Identification for Emerging Intelligent Radios: Classical Problems and New Challenges. *IEEE Instrum. Meas. Mag.* **2015**, *18*, 11–18. [[CrossRef](#)]
2. Marey, M.; Dobre, O.A. Blind Modulation Classification for Alamouti STBC System With Transmission Impairments. *IEEE Wirel. Commun. Lett.* **2015**, *4*, 521–524. [[CrossRef](#)]
3. Marey, M.; Mostafa, H. Turbo Modulation Identification Algorithm for OFDM Software-Defined Radios. *IEEE Commun. Lett.* **2021**, *25*, 1707–1711. [[CrossRef](#)]
4. Launay, F.; Perez, A. *LTE Advanced Pro: Towards the 5G Mobile Network*; Wiley: Hoboken, NJ, USA, 2019.
5. Marey, M.; Mostafa, H.; Dobre, O.A.; Ahmed, M. Data Detection Algorithms for BICM Alternate-Relaying Cooperative Systems with Multiple-Antenna Destination. *IEEE Trans. Veh. Technol.* **2016**, *65*, 3802–3807. [[CrossRef](#)]
6. Mostafa, H.; Marey, M.; Ahmed, M.H.; Dobre, O.A. Decoding Techniques for Alternate-Relaying Cooperative Systems. *EURASIP J. Wirel. Commun. Netw.* **2013**, *2013*, 236. [[CrossRef](#)]
7. Mostafa, H.; Marey, M.; Ahmed, M.; Dobre, O.A. Simplified Maximum-likelihood Detectors for Full-rate Alternate-relaying Cooperative Systems. *IET Commun.* **2013**, *7*, 1899–1906. [[CrossRef](#)]
8. Lehmann, F. A Factor Graph Approach to Iterative Channel Estimation, Detection, and Decoding for Two-Path Successive Relay Networks. *IEEE Trans. Wirel. Commun.* **2016**, *15*, 5414–5429. [[CrossRef](#)]
9. El-Malek, A.A.; Zummo, S. A Bandwidth-Efficient Cognitive Radio With Two-Path Amplify-and-Forward Relaying. *IEEE Wirel. Commun. Lett.* **2015**, *4*, 66–69. [[CrossRef](#)]
10. Zheng, J.; Lv, Y. Likelihood-Based Automatic Modulation Classification in OFDM With Index Modulation. *IEEE Trans. Veh. Technol.* **2018**, *67*, 8192–8204. [[CrossRef](#)]
11. Pathy, A.K.; Kumar, A.; Gupta, R.; Kumar, S.; Majhi, S. Design and Implementation of Blind Modulation Classification for Asynchronous MIMO-OFDM System. *IEEE Trans. Instrum. Meas.* **2021**, *70*, 5504011. [[CrossRef](#)]
12. Punchihewa, A.; Dobre, O.A.; Rajan, S.; Inkol, R. Cyclostationarity-based Algorithm for Blind Recognition of OFDM and Single Carrier Linear Digital Modulations. In Proceedings of the 2007 IEEE 18th International Symposium on Personal, Indoor and Mobile Radio Communications, Athens, Greece, 3–7 September 2007; pp. 1–5. [[CrossRef](#)]
13. Hameed, F.; Dobre, O.A.; Popescu, D.C. On the Likelihood-Based Approach to Modulation Classification. *IEEE Trans. Wirel. Commun.* **2009**, *8*, 5884–5892. [[CrossRef](#)]
14. Dobre, O.A.; Abdi, A.; Bar-Ness, Y.; Su, W. A survey of automatic modulation classification techniques: Classical approaches and new developments. *IET Commun.* **2007**, *1*, 137–156. [[CrossRef](#)]
15. Ramkumar, B. Automatic Modulation Classification for Cognitive Radios Using Cyclic Feature Detection. *IEEE Circuits Syst. Mag.* **2009**, *9*, 27–45. [[CrossRef](#)]
16. Marey, M.; Mostafa, H.; Alshebeili, S.A.; Dobre, O.A. Iterative Modulation Classification Algorithm for Two-Path Successive Relaying Systems. *IEEE Wirel. Commun. Lett.* **2021**, *10*, 2017–2021. [[CrossRef](#)]
17. Marey, M.; Mostafa, H.; Alshebeili, S.A.; Dobre, O.A. Blind Modulation Identification Algorithm For Two-Path Successive Relaying Systems. *IEEE Wirel. Commun. Lett.* **2021**, *10*, 2369–2373. [[CrossRef](#)]